p-type conductivity in GaN:Zn monocrystals grown by ammonothermal method

Maciej Zajac, Leszek Konczewicz, Elzbieta Litwin-Staszewska, M. Iwinska, R. Kucharski, Sandrine Juillaguet, Sylvie Contreras

P-type conductivity in GaN:Zn monocrystals grown by ammonothermal method

M. Zajac[1*], L. Konczewicz[1,2], E. Litwin-Staszewska[1], M. Iwinska[1], R. Kucharski[1], S. Juillaguet[2] and S. Contreras[2]

[1] *Institute of High Pressure Physics, Polish Academy of Sciences, Sokolowska 29/37, 01-142 Warsaw, Poland*

[2] *Laboratoire Charles Coulomb (L2C), University of Montpellier, CNRS, Montpellier, France.*

[*]corresponding author: zajac@unipress.waw.pl

Abstract. Zinc is often regarded as an alternative to magnesium p-type dopant in gallium nitride. However, besides many theoretical predictions, at present there are poor data on experimentally revealed p-type conductivity and evaluation of Zn activation energy by means of electrical transport measurements. In this paper ammonothermal crystallization of bulk GaN:Zn monocrystals is reported. Despite a high doping level of Zn (up to 2×10^{20} cm^{-3}), p-type conductivity with hole concentration as low as of 4×10^{15} cm^{-3} at room temperature and mobility about 3 cm^2/Vs was observed. A deep nature of the Zn acceptor was proved, as the ionization energy can exceed 260 meV. In addition, conduction in the impurity band appeared at temperature as high as room temperature.

I. Introduction.

Quantum structures based on GaN and its ternary InGaN and AlGaN alloys are suitable materials for blue and green optoelectronics [1], as well as electronic power devices of outstanding reliability and high operating voltages (above 1kV) [2,3,4]. The undisputable success in worldwide commercialization of white LEDs and blue semiconductor lasers in everyday life has been possible thanks to the achievement of effective p-type doping in GaN [5]. This aspect was highly appreciated by granting a Nobel Prize to prof. S. Nakamura, prof. H. Amano and prof. I. Akasaki in 2014 for their invention of GaN-based white LEDs.

At present, the only effective p-type dopant used in device applications is Mg substituting Ga site (Mg_{Ga}) [6,7]. Experimentally observed ionization energy of the Mg acceptor is relatively high (150-200 meV) [8]. Thus, only a small part of Mg acceptors give rise to p-type conductivity at room temperature (RT). Doping efficiency is low, but still high enough to treat Mg as the most common workable p-type dopant in GaN. In the case of GaN:Mg crystals or epitaxial layers grown by methods involving hydrogen- rich environment, the activation of Mg by high-temperature annealing is necessary [5]. According to common knowledge, this procedure removes hydrogen from electrically neutral Mg-H complexes.

In parallel, the search for other alternative p-type dopants has been carried out (Be, C and Zn). Despite the lowest reported ionization energy (113±5 meV) of Be in GaN [9], the RT p-type conductivity cannot be accomplished in GaN:Be and no p-n junctions have so far been realized utilizing Be as a p-type dopant. The main obstacle could be the strong compensation by Be interstitials [10]. In the case of carbon substituting nitrogen atoms (C_N), its acceptor level is located very high (0.9 eV) above the valence band maximum (vbm) [11]. GaN:C samples have been highly resistive at RT and p-type conductivity has been revealed only at high temperature [12]. Activation of acceptor traps of an unrecognized nature was also recently reported as an effective p-type dopant in nitride-based structures [13].

Zn substituting Ga sites (Zn_{Ga}) is considered as another possible acceptor in GaN. Zn-doped GaN is known for its intense blue luminescence (BL) peaked at about 2.8 eV [14]. The optical properties of Zn_{Ga} have been studied since the 1970s [14,15]. Zn was even used as an intentional dopant in InGaN active regions of early LEDs, giving blue emission from the InGaN/GaN structures [16]. The BL is the result of the electron transition from the conduction band or shallow donors to the acceptor level associated with Zn (so-called e-A or DAP transitions, respectively) [17]. The first ab initio calculations predicted that Zn_{Ga} in wurtzite GaN was an acceptor with binding energy 330-400 meV [18,19]. This is in agreement with the value experimentally deduced from optical spectroscopy [15]. Later calculations updated this value to 450 meV and suggested a polaronic nature of the Zn acceptor in GaN [20]. The

ionization energy of Zn is higher than that of the Mg acceptor, which reduces the importance of Zn as a viable candidate for an efficient p-type dopant. Indeed, all of the GaN:Zn samples studied so far have been n-type or highly resistive. In particular, the Zn substituting N-site (Zn_N) was proposed to explain the high resistivity, since Zn_N can accept up to three electrons from the nearest donors, making the material semi-insulating [14,21]. Several deep levels related to different charge states of Zn_N may lead to various optical transitions observed experimentally at 2.5 eV, 2.2 eV, and 1.8 eV [15]. To the best of our knowledge, there are no papers evidently showing p-type RT conductivity of bulk or epitaxial GaN:Zn. Only some recent studies on p-type Zn-doped GaN films deposited on Si(100) and glass substrates by RF reactive sputtering at 100-400 °C were reported [22]. The obtained polycrystalline films possess free hole concentration of 6.1×10^{17} cm^{-3} with the mobility of 17.7 cm^2/Vs and electrical conductivity of 1.72 S/cm at RT without any post-growth annealing. In this work we demonstrated for the first time p-type conductivity in monocrystalline bulk GaN:Zn crystals obtained by ammonothermal method in basic environment, proving experimentally that the Zn dopant can contribute to p-type conductivity in GaN. In particular, we evaluated the basic electrical properties of the examined material, including the ionization energy of the Zn acceptor.

II. Experimental.

The ammonothermal process of GaN:Zn, performed at the temperature of 450-550 °C and pressure of 200-400 MPa, took advantage of a highly reactive supercritical ammonia solution in an appropriate temperature gradient. The dissolved feedstock material (metallic Ga and Zn of 6N purity) was transported via convection to the crystallization zone, where GaN was deposited on native seeds due to supersaturation of the solution. The details of the ammonothermal method of GaN growth have been described elsewhere [23,24]. Three processes with different amount of Zn (increasing from sample #1 to #3) introduced into the autoclave were performed. The resulting as-grown *c*-plane oriented crystals (grown along the $[000\bar{1}]$-axis) were 1 mm thick and 10 mm × 15 mm in size. No post-growth annealing was performed.

Table I. SIMS analysis of chemical elements in GaN:Zn and reference ammonothermal GaN samples.

Sample	**Zn (cm^{-3})**	**O (cm^{-3})**	**H (cm^{-3})**	**Si (cm^{-3})**	**Mg (cm^{-3})**	**Mn (cm^{-3})**	**Fe (cm^{-3})**	**C (cm^{-3})**
#1	2.5×10^{19}	1.6×10^{19}	3×10^{19}	1.6×10^{18}	3×10^{16}	6.2×10^{16}	3×10^{15}	3×10^{16}
#2	6.2×10^{19}	9×10^{18}	2.3×10^{19}	9.5×10^{17}	3×10^{17}	1.1×10^{17}	7.3×10^{15}	3×10^{16}
#3	2×10^{20}	1×10^{19}	1×10^{20}	1×10^{18}	1×10^{17}	2×10^{17}	7×10^{16}	2.5×10^{16}

reference	7.3×10^{16}	1.5×10^{19}	7×10^{18}	2.3×10^{17}	7.3×10^{16}	2.5×10^{16}	7.3×10^{15}	5.2×10^{16}

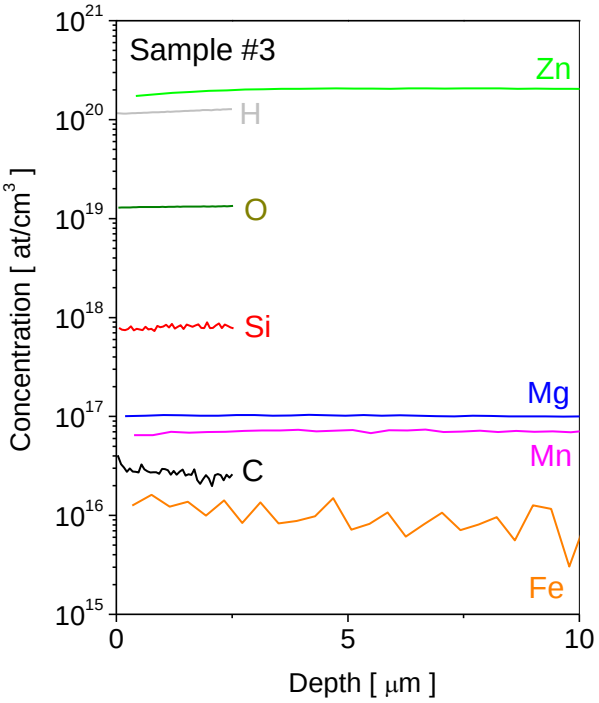

Fig. 1. Concentration of chemical elements measured as a function of bombarding ion depth by SIMS method for sample #3.

Small 5 mm × 5 mm samples were cut out from the resulting crystals for Secondary Ion Mass Spectrometry (SIMS) and electrical characterization. The SIMS measurements were performed on the N-face of the samples after polishing off at least 100 μm from the as-grown surface. The aim of such procedure was to avoid measurements on as-grown surface, on which uncontrolled deposition could occur due to the contact with ammonia solution at the process termination and during autoclave cooling. The etching depth of O^- and Cs^+ bombarding ions was up to 2.5 μm and 10 μm, respectively. This way, the depth dependence of the secondary ion count was stabilized after a possible uncontrolled surface contamination due to sample polishing. The concentrations for different elements are uniform throughout the scan depth in SIMS. A typical SIMS in-depth profile (sample #3) is presented in Fig. 1. The SIMS results of all the investigated samples are presented in Table I. It can be seen the dominating chemical element in all the investigated samples was Zn with the concentration between 2.5×10^{19} cm^{-3} in sample #1 and 2×10^{20} cm^{-3} in sample #3. Other elements with high concentrations, comparable to this of Zn, are oxygen and hydrogen. As far as oxygen has been ascertained the main donor dopant in GaN and the main unintentional impurity in ammonothermal method [24] (see the results of reference, intentionally Zn undoped n-type sample in Table I), the role of hydrogen has not yet been clearly

explained. It is generally assumed that hydrogen is an amphoteric impurity in GaN. In the case of *p*-type material with the Fermi level E_F located close to the vbm, the positive charged H^+ is stable and H acts as a donor [25]. The situation was not so evident in the samples investigated in this work. In the analysis, we neglected the presence of hydrogen, assuming that this dopant does not reveal a definite donor or acceptor character. It may also form complexes with intrinsic or extrinsic defects. The concentration of other residual elements (Si, Mg, Mn, and Fe) did not exceed ~1×10^{18} cm^{-3}. These elements, inherent to the growth process character, correspond to the unintentional impurities present in the reference, unintentionally doped sample (Table I). The concentrations of these elements (in particular Mg) are too low to control the electrical parameters of the material.

For electrical measurements the Ga-face of the 5 mm x 5 mm samples were polished mechanically, cleaned and exposed to inductively coupled plasma (ICP) non-selective etching. Ni/Au ohmic contacts in van der Pauw configuration were deposited on such a prepared surface and annealed at 500 °C for a few minutes under atmosphere of N_2 with 20% admixture of O_2. The van der Pauw method was used to measure resistivity ρ and Hall effect in a temperature range 77 – 1000K. The measurement parameters were controlled to ensure ohmic conditions.

III. Results of electron transport characterization.

The Hall carrier concentration p_H and Hall mobility μ_H can be expressed in terms of the Hall constant R_H by the following relations:

$$R_H = \frac{V_H d}{IB} = \frac{r}{p_H q} \quad (1)$$

$$\mu_H = \frac{1}{\rho p_H e} = \frac{R_H}{\rho} \quad (2)$$

where V_H is the Hall voltage, I – electric current intensity, B- magnetic field induction, ρ – resistivity, q – electron/hole charge, d - thickness of the sample, r - carrier scattering factor, in our case it was assumed to be equal to 1.

The experimental results of resistivity *vs* inverse temperature are presented in Fig. 2. For sample #3, measured in the widest temperature range (1.1<1000/*T*<12), three characteristic temperature ranges (A, B and C marked in Fig. 1) of the $\rho(T)$ dependence could be distinguished. In the higher temperature range A (1.1<1000/T<2.2) the resistivity exponentially decreased with the increasing temperature. This suggests a temperature activation of holes from the Zn acceptor to the valence band. The characteristic energy of the exponential decay (slope of the experimental $\rho(1/T)$) was determined at ~E_A=280 meV. In the lower temperature regime B (2.2<1000/T<5) the resistivity curve of sample #3 started to reduce its slope to achieve E_A~70 meV in region C (1000/T>5). An emergence of contribution of another shallower acceptor is rather impossible. The observed behavior could be explained in terms of the conduction via

hopping transport within the impurity band associated with the Zn acceptor. In highly doped samples the mean distance between the impurity atoms is low, enabling an efficient overlap between their orbital wave functions. In this way, an impurity band of the finite width is formed and holes can hop between different impurity atoms. A similar observation of hopping conductivity at relatively high temperature was published in the case of heavily Mg-doped epitaxial layers [8,26,27]. In region C, this mechanism dominated the conduction process. We assumed that the resistivity in this region obeyed the Mott's law of variable range hopping and the conduction process could be described by the phenomenological expression of resistivity:

$$\rho(T) = \rho_0 \exp\left(\frac{T_0}{T}\right)^{1/4} \qquad (3)$$

where ρ_0 is the proportionality factor and T_0 is the characteristic temperature [28]. Such a character of the $\rho(T)$ dependence is visualized in the inset of Fig. 2, where a linear behavior of resistivity vs. $T^{-1/4}$ is observed (in a logarithmic scale). In region B, both transport in valence band and hopping mechanisms coexist.

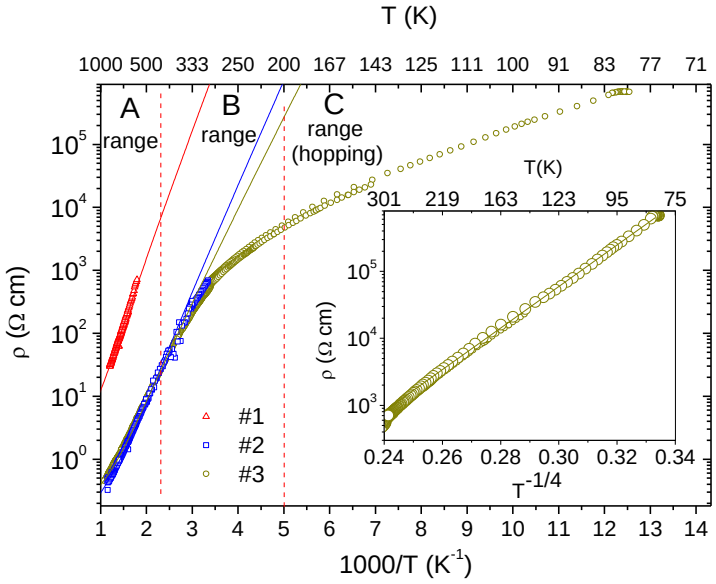

Fig. 2. Results of resistivity vs. inverse temperature measurements for samples #1, #2 and #3. Three regions of different transport mechanisms are marked and separated by red dashed lines: thermally activated conduction regime (A), hopping influenced (mixed) regime (B), hopping dominated regime (C). The solid lines represent solution of charge neutrality equation in region A (using parameters listed in Table II). The inset shows resistivity vs. $T^{-1/4}$ in region C and fit of the Mott's law (solid line). The fitting parameters in hopping regime are $\rho_o = 1.1\times10^5\,\Omega$cm; T_o=75.4 K).

The resistivity of sample #1 and #2 was measured mainly in region A (high temperature range). The resistivity of sample #2 in the whole investigated temperature range was very similar to sample #3

(with E_A=320 meV). For sample #1 it was higher by about two orders of magnitude than in sample #2, while its slope (E_A=450 meV) was higher than in the case of samples #2 and #3. This effect can be simply related to the difference of the compensation degree of the material. One can suppose that sample #1 is more compensated then sample #2 and #3 (see Zn and O concentrations in Table I).

An important point of the presented study is the temperature dependence of the Hall effect (measured for samples #2 and #3), in particular measurements of Hall effect at RT. The results from RT (possible only for sample #3) are presented in Fig. 3. The Hall voltage measurements were performed by the van der Pauw approach [29] combined with the measurements as a function of the magnetic field B varying in the range between - 0.8 T and 0.8 T. A small value of the Hall voltage (35-65 μV) results from the large thickness of the bulk sample (275 μm). The Hall carrier concentration was calculated from the slope of the Hall voltage versus B: dV_{Hall}/dB. Despite the light dispersion of the experimental points, their linear dependence on the magnetic field with a slope dV_H/dB=+0.016 mV/T does not raise doubts. The positive dV_H/dB value indicates p-type conductivity in this sample. From this slope value and the measured sample resistivity ρ=560 Ωcm the following RT parameters can be evaluated (Eq. 1 and 2): Hall hole concentration p_{Hall} = 7×10^{16} cm^{-3} and Hall hole mobility μ_H = 0.16 cm²/Vs. The low hole concentration for Zn concentration equal to 2×10^{20} cm^{-3} means poor efficiency of Zn acceptors.

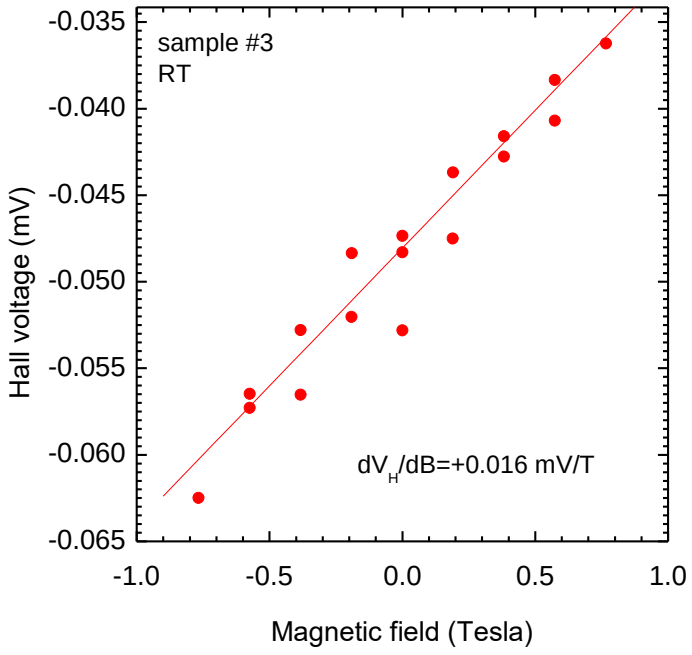

Fig. 3. The dependence of Hall voltage *vs.* magnetic field of sample #3, together with linear fit, yielding the Hall hole concentration at room temperature: p_H=7×10^{16} cm^{-3}.

The temperature dependence of the hole concentration for samples #2 and #3 is presented in Fig. 4. For both samples the concentration increased as a function of temperature to more than 1×10^{18} cm^{-3} at

T>700K. At the same time the mobility increased with temperature from ~0.1 cm^2/Vs (at RT) to a small, but rather typical of p-type GaN value of about 2-3 cm^2/V in the high temperature range (Fig. 5). We attribute the increase of experimentally observed mobility below 400 K to an artefact related to the hopping contribution in the conduction process. Taking into account the hopping contribution in mixed regime (B), we extract the free hole mobility value in the valence band (μ_V) in the whole temperature range. This mobility is temperature independent.

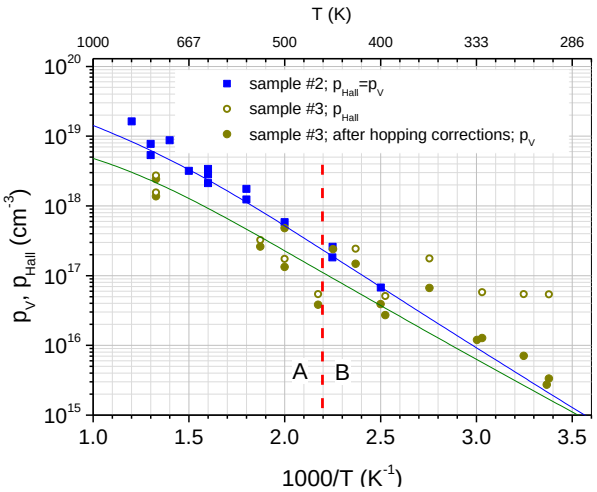

Fig. 4. Raw experimental data of Hall hole concentration p_{Hall} plotted as a function of inversed temperature (full blue rectangles for sample #2 and open green circles for sample #3) and free hole concentration p_v (full green circles) obtained by extraction of hopping contribution (only for sample #3). Solid lines represent the description by charge neutrality equation with parameters listed in Table II.

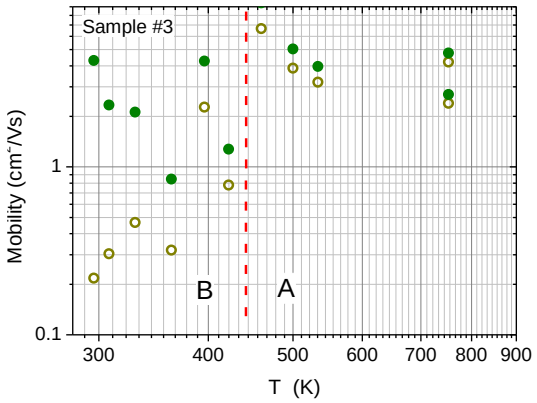

Fig. 5. Temperature dependence of mobility of sample #3 in the regions of single activation regime (A) and mixed regime (B) marked and separated by red dashed line. Open green circles correspond to the experimentally measured Hall mobility and full green circles to the extracted value of free hole mobility (μ_V) in the valence band.

IV. Hopping conductivity.

It can be seen in Fig. 2 that for temperature values close to RT the resistivity of sample #3 falls into the mixed regime and the contribution from the valence band conduction should be extracted from the raw p_{Hall} data presented in Fig. 4 and 5. The Hall coefficient in the case of two types of carriers of concentration values n_1, n_2 and corresponding mobility values μ_1, μ_2, (conductivities σ_1, σ_2), can be described as:

$$R_H = \frac{\mu_1^2 n_1 + \mu_2^2 n_2}{e(\mu_1 n_1 + \mu_2 n_2)^2} = \frac{\sigma_1^2 R_{H1} + \sigma_2^2 R_{H2}}{(\sigma_1 + \sigma_1)^2} \quad (3)$$

where e is the elementary charge and R_{Hi} - the Hall coefficient of each component $R_{Hi}=1/en_i$ (i=1,2). In our situation, we followed the analysis by Schklovskii and Efross [30] and assumed that the carriers were divided into two groups: 1) valence band holes characterized by concentration p_v, mobility μ_v and Hall coefficient R_{Hv}; 2) impurity band carriers characterized by hopping conductivity σ_h and hopping mobility $\mu_h=R_{Hh}\sigma_h$ (R_{Hh} – Hall coefficient of hopping holes). As a result, the experimentally measured Hall coefficient can be described by:

$$R_H = \frac{\sigma_v^2 R_{Hv} + \sigma_h \mu_h}{(\sigma_v + \sigma_h)^2} \quad (4)$$

We assumed further that the hopping mobility was negligible, as compared to the band mobility, so we neglected the term $\sigma_h \mu_h$ in Eq. 4. In GaN:Mg epitaxial layers the hopping mobility of about 0.001 cm^2/Vs was estimated, much lower than the band hole mobility of a few cm^2/Vs [31]. Thus, neglecting the hopping mobility (constituting 0.1% of band hole mobility) is a very reasonable approximation also in GaN:Zn.

However, the hopping carriers still contribute to the total conductivity of the sample. Consequently, the band carrier concentration can be obtained from experimental Hall coefficient:

$$p_v = \frac{1}{eR_H}\left(1 + \frac{\sigma_h}{\sigma_v}\right)^{-2} = p_{Hall}\left(\frac{\sigma - \sigma_h}{\sigma_h}\right)^2 \quad (5)$$

We assumed here that σ is the total conductivity (related to the experimental resistivity ρ): $\sigma=\sigma_h+\sigma_v=1/\rho$. To extract p_v, σ_h had to be calculated for each point of experimental p_{Hall} shown in Fig. 4. This was carried out by an extrapolation of Mott's law from the hopping region (inset in Fig. 2) to mixed (B) and single activation region (A).

The extracted p_v values for sample #3 are presented in Fig. 4 as full green circles. It can be seen that at near room temperature a correction for hopping was still substantial, while in the activation region A it was negligible, as expected. The corrected RT valence band hole concentration p_v was as low as

$(4\pm1)\times10^{15}$ cm^{-3}. Due to the larger quantity of oxygen donors (Figure 1), Mg with concentration 1-3×10^{17} cm^{-3} can be neglected as all of them should be compensated. Moreover, at high temperature the hole density far exceeds the Mg SIMS concentration, so the dominant source of holes are Zn acceptors. The extracted values of free holes mobility (sample #3) in the valence band, μ_V, are presented in Fig. 5 as full green circles. In the entire investigated temperature range the carrier mobility in the valence band can be considered constant and equal to about ~2-4 cm²/Vs. This can be understood by the fact that measured range of mobility falls into the broad maximum of its temperature dependence, where both effects of ionized impurities and phonon scattering are important. A similar behavior was observed in the case of low mobility GaN:Mg layers [26].

V. Discussion.

The hole concentration p_v (samples #2 and #3) and resistivity (samples #1, #2nd ad #3) can be tentatively described in the frame of the carrier occupation statistics. The measured p_v can be described by a numerical solution of the charge neutrality equation [32] in the form:

$$p_v + N_{DO}^{+} = n_c + N_{AZn}^{-} = n_c + \frac{N_{Zn}}{1+g_{Zn}\cdot\exp(\frac{E_{Zn}-E_F}{k_BT})} \qquad (6)$$

where p_v and n_c are concentration of holes and electrons (in our case n_c is negligible, since all donors act as compensating centers and do not provide electrons to the conduction band) in the valence and conduction bands, respectively, N_{DO}^{+} – concentration of ionized oxygen donors (equal to concentration of neutral donors N_{DO}, since all donors compensate acceptor states),N_{Zn}^{-} - concentration of ionized Zn acceptors, g_{Zn} is the degeneracy factor of the Zn acceptor level. An important parameter of this analysis is the Zn acceptor ionization energy E_{Zn} with respect to the vbm.

The solid lines in Figs. 2 and 4 represent the description of the inverse temperature dependence of resistivity and valence band hole concentration, respectively. In unintentionally doped with oxygen n-type ammonothermal GaN (of oxygen concentration 1-2×10^{19} cm^{-3}) the free electron concentration follows the oxygen content [24]. Thus, in the first approach we assigned and fixed the N_{D0} parameter with the SIMS oxygen concentration (Table I). Then, we described the experimental $p_v(T)$ and $\rho(T)$ using N_{Zn} and E_{Zn} as the fitting parameters. The calculations were done using the parameters listed in Table II. The g_{Zn} parameter was assumed to equal 1 and the mean hole effective mass $m_h^*=1.5m_0$ (m_0 –free electron mass) [33]. We further assumed that the location of the Zn acceptor level with respect to the vbm did not change with temperature. When modeling the resistivity, it was assumed that the mobility of holes in the valence band was constant and independent of temperature. The highest E_{Zn}=350 meV was observed for the most compensated sample #1. The ionization energy was lower for samples #2 and

#3 (300 meV and 260 meV, respectively). Such a decrease of ionization energy may be a consequence of electrostatic interaction screening by impurities, as observed in heavily doped GaN:Mg [34]. Such a hypothesis was confirmed by the observation of hopping transport in sample #3. The obtained N_{Zn} values were similar to the Zn content measured by SIMS for samples #1 and #2, while the calculated N_{Zn} was much lower than the SIMS value for sample #3. We speculate that this effect could be due to a decrease of the Zn doping efficiency (at Ga-sites) with increasing the doping level (Zn amount introduced into the growth zone). It seems that the doping efficiency was optimal for sample #2. However, this phenomenon requires further detailed research.

Table II. Parameters obtained by modeling of $p_v(T)$ and $\rho(T)$ experimental data by carrier occupation statistics (Eq. 6). Theoretical p_v at RT is also given. For benchmarking purpose literature data for GaN:Mg are provided [26,27,34] in the last column (N_A-N_D – effective density of acceptors, E_{Mg} – ionization energy of Mg acceptor).

	Sample #1	**Sample #2**	**Sample #3**	**GaN:Mg (benchmark)**
N_{DO} (fixed) (cm^{-3})	1.6×10^{19}	9×10^{18}	1×10^{19}	-
N_{Zn} (SIMS) (cm^{-3})	2.5×10^{19}	6.2×10^{19}	2×10^{20}	1×10^{18}-1×10^{20} (N_A-N_D)
N_{Zn} (model) (cm^{-3})	$(1.70\pm0.03)\times10^{19}$	$(6.2\pm0.5)\times10^{19}$	$(3\pm1)\times10^{19}$	1×10^{18}-1×10^{20} (N_A-N_D)
E_{Zn} (meV)	350±5	300±10	260±20	E_{Mg}=50-220
p_v at RT (cm^{-3})	2×10^{13}	3×10^{15}	1.7×10^{15}	5×10^{16}-1×10^{19}
μ_v at RT (cm^2/Vs)	2.2	1.4	3.3	< 60

It should be underlined that the ionization energy of Zn impurity value and other fitting parameters used in the calculations must be handled with care. One should bear in mind that there are

still many open questions that may have a large impact on the real parameters N_A and N_D. Firstly, not all the incorporated Zn atoms may occupy Ga-sites, as mentioned earlier. The location of Zn at N-sites cannot be excluded [15,21]. Secondly, it is not known how other point defects (intrinsic or extrinsic) influence the electrical properties of GaN:Zn. In particular, the role of hydrogen is not clarified. Nevertheless, the deep nature of the Zn acceptor contributing to p-type conductivity was experimentally confirmed with the value of acceptor binding energy E_{Zn} about 350 meV. The range of experimentally determined ionization energy of the Zn acceptor contains higher values than the reported for GaN:Mg [26,34], while the RT hole concentration is significantly lower (Table II). Precise values of ionization energies should be determined after a more detailed investigation, including photoluminescence, capacitance-voltage, and others.

VI. Summary.

To summarize, the electrical properties of bulk GaN:Zn grown by ammonothermal method were studied. In the examined samples, Zn was the dominant acceptor and it gave rise to p-type conductivity observed at RT and elevated temperatures. The conduction activation process could be described by the energy position of the Zn_{Ga} acceptor level higher than 260-280 meV above vbm. The ionization energy of Zn was larger than typical values obtained for Mg in GaN crystals [8,34]. As a consequence, despite a high doping level, a very low hole concentration of 4×10^{15} cm^{-3} was observed at RT. RT resistivity of 1×10^{3} Ωcm was measured, which corresponded to very low mobility (~3 cm^2/Vs). In addition, the observation of hopping conductivity indicated the formation of a broad impurity band. It seems that although Zn gives undoubtedly p-type doping, its technological use is challenging.

Acknowledgements:

This research was supported by TEAM TECH program of the Foundation for Polish Science co-financed by the European Union under the European Regional Development Fund (POIR.04.04.00-00-5CEB/17-00) as well as by the Polish National Science Center through projects No. 2020/37/B/ST5/03746 and 2018/29/B/ST5/00338.

We are very grateful to dr Ryszard Piotrzkowski for numerous and very helpful discussions.

Data availability

The data that support the findings of this study are available from the corresponding author upon reasonable request.

References:

[1] T. D. Moustakas, Roberto Paiella, Rep. Prog. Phys. **80** 106501 (2017).

[2] H. Amano et al., J. Phys. D: Appl. Phys. **51** 163001(2018).

[3] P. Shrestha, M. Guidry, B. Romanczyk, N. Hatui, Ch. Wurm, A. Krishna, S. S. Pasayat, R. H. Karnaty, S. Keller, J. F. Buckwalter, U. K. Mishra, IEEE Electron Device Letters **41**, 681-684 (2020).

[4] B. Romanczyk, W. Li, M. Guidry, N. Hatui, A. Krishna, Ch. Wurm, S. Keller, U. K. Mishra, IEEE Electron Device Letters **41**, 1633-1636 (2020).

[5] S. Nakamura et al., T. Mukai, M. Senoh, N. Iwasa, Jpn. J. Appl. Phys. **31**, L139 (1991).

[6] A. Krishna, A. Raj, N. Hatui, S. Keller, U. K. Mishra, Appl. Phys. Lett. **115**, 172105 (2019).

[7] A. Krishna, A. Raj, N. Hatui, O. Koksaldi, R. Jang, S. Keller, U. K. Mishra, Phys. Status Solidi A **217**, 1900692 (2020).

[8] W. Gotz, N. M. Johnson et al., Semiconductors and Semimetals **57**, 185 (1998).

[9] D. O. Demchenko, M. Vorobiov, O. Andrieiev, T. H. Myers, M. A. Reshchikov, Phys. Rev. Lett. **126**, 072401 (2021).

[10] C. G. Van de Walle, S. Limpijumnong, J. Neugebauer, Phys. Rev. B **63** 245205 (2001).

[11] J. L. Lyons, A. Janotti, and C. G. Van de Walle, Phys. Rev. B 89, 035204 (2014).

[12] M. Iwinska, R. Piotrzkowski, E. Litwin-Staszewska, T. Sochacki, M. Amilusik, M. Fijalkowski, B. Lucznik, and M. Bockowski, Appl. Phys. Express 10, 011003 (2017).

[13] A. Krishna, A. Raj, N. Hatui, I. Sayed, S. Keller, U. K. Mishra, Appl. Phys. Lett. **117**, 042104 (2020).

[14] J. Pankove, J. A. Hutchby, Appl. Phys. Lett. **24** 281(1974).

[15] B. Monemar, O. Lagerstedt, H. P. Gislason, J. Appl. Phys. **51** 640 (1980).

[16] S. Nakamura, J. Crystal Growth **145**, 911 (1994).

[17] M. A. Reshchikov, H. Morkoc, J. Appl. Phys. **97**, 061301 (2005).

[18] F. Mireles, S. E. Ulloa, Phys. Rev. B **58**, 3879 (1998).

[19] H. Wang, A. B. Chen, Phys. Rev. B **63**, 125212 (2001).

[20] J. L. Lyons, A. Janotti, C. G. Van de Walle, Jpn. J. Appl. Phys. **52** 08JJ04 (2013).

[21] Ł. Janicki, M. S. Mohajerani, J. Hartmann, E. Zdanowicz, H. H. Wehmann, A. Waag, R. Kudrawiec, Appl. Phys. Lett. **113,** 032109 (2018).

[22] T. T. Anh Tuan, D. H. Kuo, A. D. Saragih, G. Z. Li, Mat. Sci. Eng. B, **222,** 18 (2017).

[23] R. Dwilinski. R. Doradzinski, J. Garczynski, L. P. Sierzputowski, A. Puchalski, Y. Kanbara, K. Yagi, H. Minakuchi, H. Hayashi, J. Crystal Growth, **311**, 3015 (2009).

[24] M. Zajac, R. Kucharski, K. Grabianska, A. Gwardys-Bak, A. Puchalski, D. Wasik, E. Litwin-Staszewska, R. Piotrzkowski, J.Z Domagala, M. Bockowski, Prog. Cryst. Growth Charact. Mater. **64**, 63 (2018).

[25] D. Andiwijayakusuma, F. Ishii, and M. Saito, Recent Development in Computational Science (Kanazawa University, 2015), Vol. 6, pp. 86–93.

[26] P. Kozodoy, H. Xing, S. P. DenBaars, U. K. Mishra, J. Appl. Phys. **87**, 1832 (2000).

[27] L. Konczewicz, S. Juillaguet, E. Litwin-Staszewska, R. Piotrzkowski, H. Peyre, S. Matta, M. Al Khalfioui, M. Leroux, B. Damilano, J. Brault, and S. Contreras, J. Appl. Phys **128**, 085703 (2020).

[28] N. F. Mott, The Philosophical Magazine: A Journal of Theoretical Experimental and Applied Physics, **19:160**, 835-852 (1965).

[29] M. Levy and M.P. Sarachik, Rev.Sci.Instrum., 60, n° 7, pp.1342-1343, 1989.

[30] B. I. Schklovskii, A. L. Efros, *Electronic Properties of Doped Semiconductors*, Springer-Verlag, p. 81 (1984).

[31] Y. Kajikawa, Physica Status Solidi (c) 14 (2017) 1600129

[32] N. W. Ashcroft, N. D. Mermin, *Solid State Physics*, Holt, Rinehart and Winston (1976).

[33] V. Bougrov, M. Levinshtein, S. Rumyantsev, and A. Zubrilov, in Properties of Advanced Semiconductor Materials: GaN, AlN, InN, BN, SiC, SiGe, edited by M. E. Levinshtein, S. L. Rumyantsev, and M. S. Shur (John Wiley & Sons, Inc., New York, 2001), p. 7.

[34] S. Brochen, J. Brault, S. Chenot, A. Dussaigne, M. Leroux, B. Damilano, Appl. Phys. Lett. **103** 032102 (2013).